Dark Photorefractive Spatial Solitons and Photorefractive Vortex Solitons

Galen Duree,[1] Matthew Morin,[1] and Gregory Salamo,[1]
Mordechai Segev,[2] Bruno Crosignani,[3] Paolo Di Porto,[3] Edward Sharp,[4] and Amnon Yariv[5]
[1]*Physics Department, University of Arkansas, Fayetteville, Arkansas 72701*
[2]*Electrical Engineering Department and Advanced Center for Photonics and Optoelectronic Materials (POEM) and Princeton Material Institute (PMI), Princeton University, Princeton, New Jersey 08544*
[3]*Dipartimento di Fisica, Universitá dell'Aquila, L'Aquila, Italy*
[4]*Army Research Laboratory, Fort Belvoir, Virginia 22060*
[5]*California Institute of Technology, Pasadena, California 91125*
(Received 30 June 1994)

We report on the first experimental observations of dark, planar, spatial photorefractive solitons, and photorefractive vortex solitons that are trapped in a bulk (three-dimensional) photorefractive media. Both the dark and vortex solitons possess the "signatures" of the photorefractive solitons: they are independent of absolute intensity, can afford significant absorption, and are inherently asymmetric with respect to the transverse dimensions of trapping.

PACS numbers: 42.50.Rh

Spatial solitons in photorefractive (PR) materials [1] have been the object of growing interest during the last two years. Thus far, three different types of PR solitons have been investigated. The first type of PR soliton which has been studied stems from the nonlocal nature of the photorefractive effect, as manifested in the dependence of the perturbation in the refractive index on the transverse derivatives of the light intensity distribution [1,2]. This type of PR soliton [3–6] exists when an external voltage is applied to the PR material, after the index gratings have been formed, but before the external field is screened by the background conductivity. Solitons of this type are transient by nature and we refer to their time window of existence as quasi-steady-state. Their most distinct properties are (i) independence of the absolute light intensity [1–3] (for intensities much larger than the dark irradiance) and (ii) the capability of trapping in two transverse dimensions [3–5]. The second type of PR soliton, which we call the screening soliton [7], appears in the steady state after the external field is screened, nonuniformly, due to the transversely nonuniform intensity distribution. This effect is local and results in an index perturbation that is inversely proportional to the sum of the optical and dark irradiances. Its most distinct properties are (i) dependence on the ratio between the optical and dark irradiances and convergence to the narrowest size for large ratios and (ii) existence of bright solitons for a negative perturbation in the index while dark solitons require a positive perturbation in the index while dark solitons require a positive perturbation (this implies that the polarity of the applied field is *opposite* to the polarity required to generate PR solitons of the first type). The third type of PR soliton is present in materials that are both photorefractive and photovoltaic. These photovoltaic solitons [8] stem from photovoltaic currents that generate (in steady state) an index perturbation analogous to the nonlinearity in a saturable absorber (sometimes called a thresholding nonlinearity), which is a local effect as well. Their most distinct property is the dependence on the ratio between the optical and dark irradiances, the narrowest solitons being obtained when this ratio is between 1 and 2.

In this Letter we report on the first experimental observation of photorefractive dark solitons and vortex solitons, both belonging to the first (nonlocal) type.

Photorefractive solitons of the first type evolve when diffraction is exactly balanced by self-scattering (two-wave mixing) of the spatial (plane wave) components of the soliton beam [1,2]. Intuitively, self-trapping occurs when diffraction (which involves accumulation, by each plane wave component of a beam, of a phase that is linear in the propagation distance) is balanced by nonlinear phase coupling that leaves the complex amplitudes of the plane-wave components unchanged. Photorefractive gratings, however, typically give rise to amplitude coupling (energy-exchange interaction) due to a dominant diffusion transport mechanism for the redistribution of the photogenerated charge carriers. Inherently, this process cannot compensate for diffraction since it alters the amplitudes of the plane-wave components rather than balancing their phases. The presence of an external bias field, on the other hand, results in strong phase coupling and is, therefore, required for the formation of these PR solitons. Our recent observations of photorefractive bright solitons of the first type [3,4] revealed that, unlike the Kerr-like solitons, the PR solitons may be trapped in two transverse dimensions and maintain their stability. We also presented experimental results [5] addressing the two-dimensional problem and pointed out that the trapping is inherently asymmetric with respect to the two transverse dimensions. We have shown experimentally that the self-trapping effects in the direction parallel to the external electric field (x direction) exist regardless of the size of the beam in the other transverse di-

 0031-9007/95/74(11)/1978(4)$06.00

mension (y). Self-trapping in the y direction (perpendicular to the field), on the other hand, is generated by tilted gratings and fully depends on the finite extent of the beam in the x direction. In this spirit, we have demonstrated that sheet solitons (of a single transverse dimension) exist along x but *not* along y, and concluded that trapping in x is independent of trapping in y but *not* vice versa. The intuitive reason is that the influence of the external field is maximal for gratings whose **K** vectors are parallel (or antiparallel) to its direction, and vanishes for gratings that are perpendicular to it. Consequently, a beam that is narrow in one transverse dimension but very wide (virtually uniform) along the other direction exhibits two, essentially different, behaviors depending whether the direction along which it is uniform coincides with that of the applied field or is orthogonal to it.

We used the experimental setup shown in Fig. 1. The solitons are observed in a quasi-steady-state, which is the time window between the formation of the (space-charge) electric field grating and the screening of the applied field. By using low intensities (I_0, the initial intensity, is 300 MW/cm^2 and the optical power is 3 μW in all the following experiments, unless specified otherwise) and minimizing beam fanning [9], this quasi-steady-state time window exceeds 2 sec in our rhodium-doped SBN:60. We identify the directions parallel and perpendicular to the direction of the external voltage with the transverse x and y axes, respectively, and recall [3,5,6] that they correspond to the crystalline **c** and **a** axes, respectively. In all the experiments the beam is extraordinarily (x) polarized.

To observe the planar dark solitons, we launch a dark notch with the necessary π phase jump in its center by inserting a thin glass slide in one half of the beam. The phase is adjusted (until the notch is obtained) by tilting the glass slide. The beam is then focused and enters the PR crystal with a notch size of 21 μm (FWHM). The output beam is split and monitored by a photodetector (to locate the quasi-steady-state time window), by a charge coupled device camera (after an imaging system

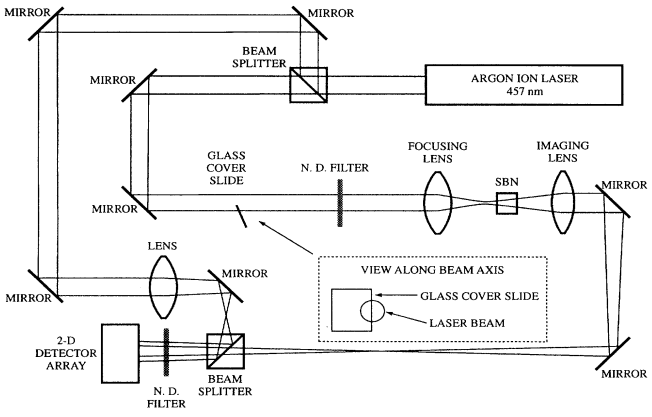

FIG. 1. The experimental setup.

[3,5,6]), and a portion of it is recombined with a portion of the original beam for an interferometric measurement. The experimental observations are shown in Figs. 2–4. Figure 2 shows the transverse profiles of the beam as it propagates through the crystal. In the left column the beam simply diffracts (zero applied field): Both the bright lobes and the dark notch increase their sizes in the same manner (from 21 μm at the input face to 35 μm at the exit face, FWHM of the notch). When a *negative* voltage is applied ($V/d \approx -400$ V/cm, where V and d are the external voltage and the crystal width, i.e., distance between the electrodes, respectively), the dark notch maintains its size and shape, while the bright lobes increase (double) their diffraction (right column). This is a good indication that the PR crystal behaves (in the quasi-steady-state) as a self-defocusing medium when a negative voltage is applied. Figure 3 displays the results of the interferometric measurement after the beam has passed through the crystal. It is evident that when the slide is absent [Fig. 3(a)] or adjusted with no phase jump across the beam [Fig. 3(b)] the interference fringes are continuous. When the slide is adjusted for a phase jump, one observes the discontinuity of the fringes at the center of the notch both for normal diffraction [Fig. 3(c)] and when the proper negative voltage is applied [Fig. 3(d)]. Having demonstrated the existence of a planar dark soliton, we proceed to test the characteristic properties of PR solitons of the first type. Figure 4 displays the beam profiles at the exit face for normal diffraction [Fig. 4(a)] and for

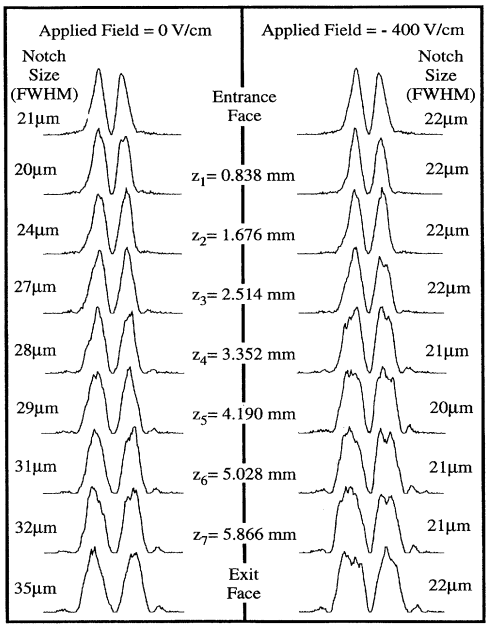

FIG. 2. Transverse profiles of the diffracting beam (left column) and the dark soliton (right column) as they propagate through the crystal. The wave forms are normalized to the maximal amplitudes, and the size of the dark notch (FWHM) is given for each plane.

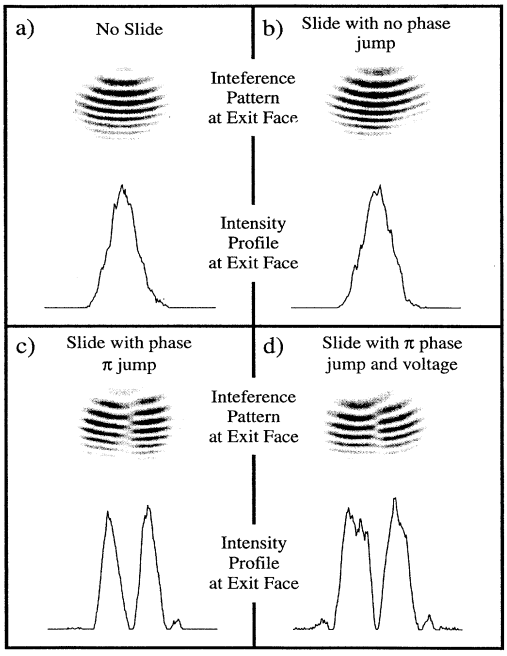

FIG. 3. Transverse beam profiles at the output plane of the crystal, and their corresponding interferograms that manifest the continuous phase for a Gaussian input beam [(a) and (b)] and the π phase jump at the origin for the diffracted notch (c) and the dark soliton (d).

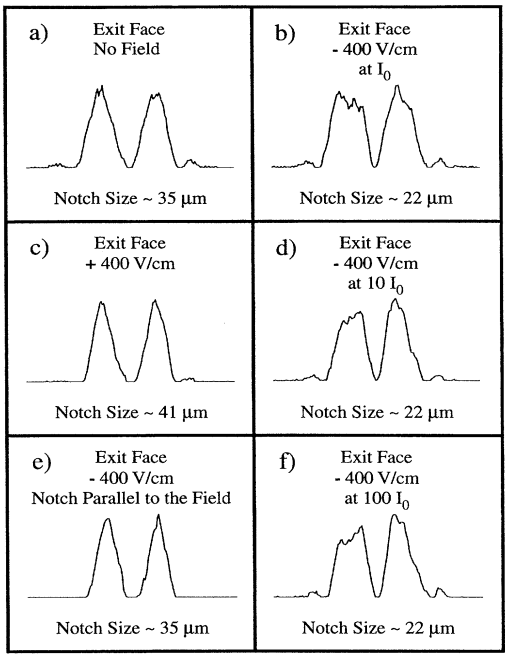

FIG. 4. Transverse beam profiles at the output plane of the crystal for normal diffraction (a), for a dark soliton at I_0, 10 I_0, and 100 I_0 (b), (d), (f), for the case of self-focusing [at positive voltages, (c)] and for a $\pi/2$ rotated notch that cannot be self-trapped (e).

a dark soliton [at $V/d \approx -400$ V/cm, Fig. 4(b)]. When we reverse the polarity of the applied field the notch increases its size significantly while the bright lobes reduce their cross sections [Fig. 4(c)]. This is a good indication that for the positive polarity of the field the PR crystal behaves as a self-focusing medium (which is suitable for trapping a bright soliton but not a dark one). An important signature of nonlocal PR solitons is their independence of the absolute light intensity. To verify this we vary the input power over 2 orders of magnitude [3–300 μW (intensities of 0.3–30 W/cm^2) for the current experiment of dark solitons, and 0.5–785 μW (intensities of 0.05–78.5 W/cm^2) for a similar experiment with bright solitons], and observed no change in the shape or the size of the dark soliton. Figures 4(d) and 4(f) show typical soliton beam profiles at 30 and 300 μW power, respectively. Note that the time window for the observation of the soliton is inversely proportional to the optical intensity which (since the soliton shape is constant within this entire range) is proportional to the optical power. Although the lower limit of this intensity region should be the dark irradiance, we are unable to reach it due to detector array limitations (we estimate the dark irradiance to be much smaller than 10 mW/cm^2). The upper limit of the intensity range is determined by thermal effects which induce nonuniformities in the index (the upper limit may be extended using temperature control). All these observations confirm that the observations are of PR solitons of the first type. Finally, we rotate the input notch, so that its cross section is now in the y direction (perpendicular to the external field). As clearly seen in Fig. 4(e), self-trapping effects of the notch cannot be observed even at higher fields (-1000 V/cm, much higher negative fields simply depole the crystal). As in the case of the bright soliton [5], this observation indicates that a beam (or a notch) that is uniform in the direction parallel to the external field *cannot* be trapped. We conclude this section by stating that we have demonstrated a planar dark PR soliton of the first (nonlocal) type. For comparison with previous theoretical analyses [10] and observations [11] of spatial Kerr-like dark solitons we point out the major differences in the properties between Kerr-like and PR solitons: (i) independence of the PR solitons on the light intensity, including the absence of a threshold, (ii) the dependence of the PR solitons on the direction of trapping (a manifestation of the tensorial nature of the PR effect), (iii) the possibility of switching from a regime of dark PR soliton to bright PR soliton regime simply by reversing the polarity of the applied field, and (iv) the stability of spatial PR solitons (both dark and bright) to trapping in two transverse dimensions.

Next, we describe the observation of PR vortex solitons. Optical vortices [12,13] are beams possessing a uniform amplitude and a phase that varies as $\exp(im\theta)$ (referring to a transverse, polar, coordinate system of r and θ), where m is an integer (called the topological

charge). Vortices on Gaussian beams [12] also exhibit a radial Gaussian dependence, and are nearly identical to the familiar "donut mode" [14] of a laser, that are often observed when the intracavity aperture of a laser is large [15]. This kind of mode can be represented as a Laguerre-Gauss mode of $p = 1$ and azimuthal dependence $\exp(im\theta)$, where $m \geq p$. We used the experimental setup shown in Fig. 1 (excluding the glass slide), and adjusted the intracavity laser aperture to launch the donut mode. Our results are shown in Fig. 5, where the horizontal (left column) and vertical (middle) cross sections of the cylindrical beam are shown together with the actual photographs (right column, darker regions represent regions of higher optical intensity), under various conditions. The upper and middle sets show the beam profiles at the entrance and exit faces of the crystal with no applied voltage. It is apparent that the bright and dark regions diffract in the same manner. When a negative voltage is applied (lower profiles) the central two-dimensional region (the optical vortex) becomes self-trapped, while the bright regions increase their diffraction significantly (indicative of the self-defocusing behavior). Note that, while the vortex is trapped in the same manner in both transverse dimensions, the diffraction of the bright regions is more enhanced in the horizontal direction. The capability to self-trap both directions symmetrically is a manifestation of the nonunique solution of the PR solitons (of the first type) with respect to the external voltage [1–3,5]. We expect, however, that if we break this symmetry in the input beam, in a manner similar to the experiment of Ref. 5, self-trapping effects will persist only in the direction parallel to the external field. Comparison to observations of optical vortex solitons in Kerr media [13] reveal that all the differences in the properties of both types, as discussed above for dark solitons, persist for the vortex solitons.

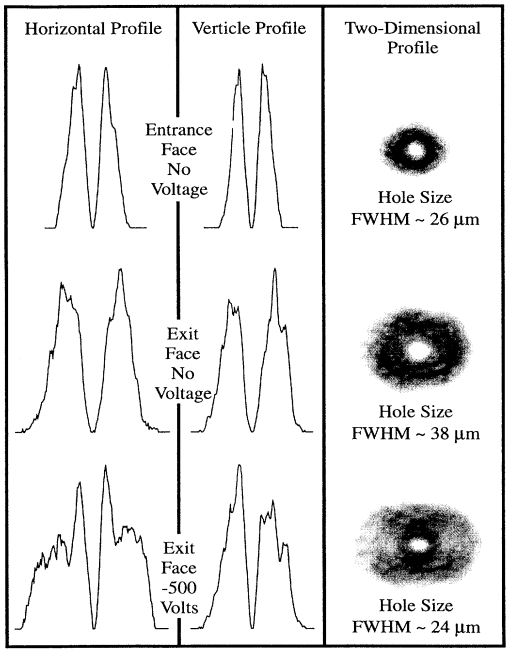

FIG. 5. Two-dimensional transverse profiles and photographs of the input (upper) and diffracting optical vortices (middle) and of the photorefractive vortex soliton (lower).

In conclusion, we have reported the first observations of photorefractive dark spatial solitons [16] and vortex solitons, and compared their properties to those of similar solitons in Kerr-like media.

[1] M. Segev, B. Crosignani, A. Yariv, and B. Fischer, Phys. Rev. Lett. **68**, 923 (1992).
[2] B. Crosignani, M. Segev, D. Engin, P. DiPorto, A. Yariv, and G. Salamo, J. Opt. Soc. Am. B **10**, 446 (1993).
[3] G. Duree, J. L. Shultz, G. Salamo, M. Segev, A. Yariv, B. Crosignani, P. DiPorto, E. Sharp, and R. R. Neurgaonkar, Phys. Rev. Lett. **71**, 533 (1993).
[4] M. Segev, A. Yariv, G. Salamo, G. Duree, J. Shultz, B. Crosignani, P. DiPorto, and E. Sharp, Opt. Phot. News **4**, 8 (1993).
[5] G. Duree, G. Salamo, M. Segev, A. Yariv, B. Crosignani, P. DiPorto, and E. Sharp, Opt. Lett. **19**, 1195 (1994).
[6] M. Segev, A. Yariv, B. Crosignani, P. DiPorto, G. Duree, G. Salamo, and E. Sharp, Opt. Lett. **19**, 1296 (1994).
[7] M. Segev, G. C. Valley, B. Crosignani, P. DiPorto, and A. Yariv, Phys. Rev. Lett. **73**, 3211 (1994).
[8] G. C. Valley, M. Segev, B. Crosignani, A. Yariv, M. M. Fejer, and M. Bashaw, Phys. Rev. A **50**, 4457 (1994).
[9] See the footnote in Ref. [6] (assigned as Ref. 6 there).
[10] V. E. Zakharov and A. B. Shabat, Zh. Eksp. Teor. Fiz. **64**, 1627 (1973) [Sov. Phys. JETP **37**, 823 (1973)].
[11] G. A. Swartzlander, D. R. Andersen, J. J. Regan, H. Yin, and A. E. Kaplan, Phys. Rev. Lett. **66**, 1583 (1991).
[12] G. S. McDonald, K. S. Syed, and W. J. Firth, Opt. Commun. **94**, 469 (1992).
[13] A. E. Siegman, *Lasers* (University of Science Books, Mill Valley, California, 1986), Chap. 17, p. 689–690.
[14] G. A. Swartzlander and C. T. Law, Phys. Rev. Lett. **69**, 2503 (1992).
[15] In some lasers the donut mode is an incoherent superposition of the Cartesian TEM_{01} and TEM_{10} modes, which cannot be used to launch a vortex soliton. When such an "incoherent" donut is used, only the mode with intensity variations parallel to the external field is trapped (at higher voltage), while the other mode remains unchanged, in agreement with the results on the planar dark soliton of Figs. 4(b) and 4(e). To emphasize this argument, we constructed an input beam that consisted of two, coherent and orthogonal to each other, dark notches (simulating Cartesian TEM_{01} and TEM_{10} modes) at a relative phase of $\pi/2$ (which is identical to the Laguerre-Gauss mode), and observed the evolution and trapping (similar to Fig. 5) of a vortex soliton from this specific input beam.
[16] We have also presented a photograph of a photorefractive dark spatial soliton on the cover page of Optics and Photonics News, volume 5, December 1994 and in the summary on page 9.

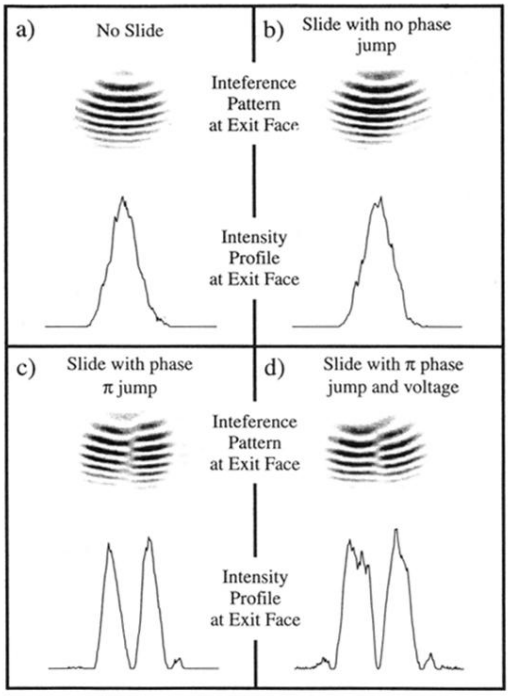

FIG. 3. Transverse beam profiles at the output plane of the crystal, and their corresponding interferograms that manifest the continuous phase for a Gaussian input beam [(a) and (b)] and the π phase jump at the origin for the diffracted notch (c) and the dark soliton (d).

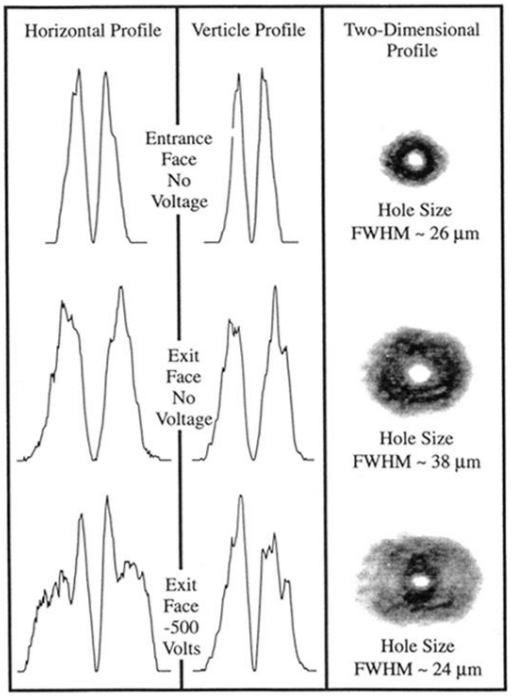

FIG. 5. Two-dimensional transverse profiles and photographs of the input (upper) and diffracting optical vortices (middle) and of the photorefractive vortex soliton (lower).